

Generative Example-Based Explanations: Bridging the Gap between Generative Modeling and Explainability

Philipp Vaeth^{1,2}, Alexander M. Fruehwald¹, Benjamin Paassen², Magda Gregorova¹

¹Center for Artificial Intelligence (CAIRO),
Technical University of Applied Sciences Würzburg-Schweinfurt, Franz-Horn-Straße 2, Würzburg, Germany
²Bielefeld University, Universitätsstraße 25, Bielefeld, Germany

Abstract

Recently, several methods have leveraged deep generative modeling to produce example-based explanations of decision algorithms for high-dimensional input data. Despite promising results, a disconnect exists between these methods and the classical explainability literature, which focuses on lower-dimensional data with semantically meaningful features. This conceptual and communication gap leads to misunderstandings and misalignments in goals and expectations. In this paper, we bridge this gap by proposing a novel probabilistic framework for local example-based explanations. Our framework integrates the critical characteristics of classical local explanation desiderata while being amenable to high-dimensional data and their modeling through deep generative models. Our aim is to facilitate communication, foster rigor and transparency, and improve the quality of peer discussion and research progress.

Code & Data — github.com/cairo-thws/XAIDIFF

Model Weights — huggingface.co/cairo-thws/XAIDIFF

1 Introduction

As more AI applications get introduced into our daily lives, the need for trust, safety and ethical use of AI in these automated decision systems increases (Goodman and Flaxman 2017; Chatila et al. 2021). Explainable Artificial Intelligence (XAI) is a research field that addresses these concerns of trust, transparency and fairness by supplementing decisions with explanations (Gunning 2017).

One popular approach - so-called *local* explanations - focuses on explaining the decision of an algorithm for a specific input data point (Adadi and Berrada 2018). A classical example originating from Wachter, Mittelstadt, and Russell (2017) is the following: "You are denied a loan. Explanation: Your income is £30,000, if it were £45,000 the loan would be granted." Such example-based explanations have been well explored in the literature (Verma et al. 2022) in the context of tabular data and are commonly known as *counterfactual explanations*.

Unfortunately, transferring techniques for example-based explanations from tabular data to high-dimensional data such as images is not straightforward. Without careful control, changes in the original pixel space may distort the image, rendering it unrealistic and hence difficult to interpret

by the user. Motivated by the field of generative modeling, we posit that one of the critical desiderata of example-based explanations is that of **fidelity** to the underlying data distribution (Delaney, Greene, and Keane 2021).

While methods for producing high-fidelity counterfactual explanations in the image domain have been suggested before (Guidotti 2022; Augustin et al. 2022; Jeanneret, Simon, and Jurie 2022), these are mostly ad-hoc and lack systematic grounding. This is due to misunderstandings between the fields of generative modeling and explainability and results in different terminology, definitions and evaluation procedures. The contribution of our paper is to bridge this gap through a novel **probabilistic framework for high-fidelity explanatory examples**, consisting of the following parts:

- **Definitions** (section 2) for *counterfactual explanations* as nearby, high-fidelity examples that change the algorithm decision; *adversarial examples* as nearby, low-fidelity examples that change the algorithmic decision; and a novel complementary concept - named *affirmative explanations* - that shall re-affirm the user understanding by providing other nearby high-fidelity examples consistent with the original decision of the algorithm.
- Translation of our definitions into the **generative explanation problem** (section 2.2) and *linking this approach into a unified view* with the previously proposed optimization problem for finding counterfactual examples for tabular data (Wachter, Mittelstadt, and Russell 2017).
- **Quantitative evaluation schema** (section 2.3) directly linked to our definitions.

We further complement our framework by:

- **A synthetic data set** (section 4.2) for a controlled explanation environment with varying complexity and intuitively unambiguous explanations.
- **A generative algorithm and its re-usable implementation** (section 3), showcasing the use of the framework in a constructive manner when developing new methods for generating explanatory examples.

2 Explanatory examples

Example-based explanations are well established in the local explainability domain, with *counterfactual explanations* as the most prominent type (Adadi and Berrada 2018; Das

and Rad 2020). The purpose of these is to help the user understand the decisions of an algorithm for a specific data example (local explanation). By applying a minimal change to the original example which changes the algorithmic decision, the user shall understand which crucial changes separate the original example from the other class according to the classifier.

The first and most famous counterfactual explanation system for tabular data was proposed by Wachter, Mittelstadt, and Russell (2017). For an original data point \mathbf{x}^* labeled by an algorithm f_θ as y_o ('o' - original), a counterfactual explanation is a point $\hat{\mathbf{x}}$ close to \mathbf{x}^* that is labeled by f_θ as y_t ('t' - target). The counterfactual $\hat{\mathbf{x}}$ can be found through the following minimization problem:

$$\min_{\hat{\mathbf{x}}} \lambda (f_\theta(\hat{\mathbf{x}}) - y_t)^2 + d(\mathbf{x}^*, \hat{\mathbf{x}}) , \quad (1)$$

with λ a hyperparameter trading off the distance d with label accuracy.

A related concept primarily explored in the image domain is that of *adversarial examples* (Goodfellow, Shlens, and Szegedy 2015), which are humanly indistinguishable variants of an original example which nonetheless are classified differently.

Note that the definitions of counterfactuals and adversarial examples, as given above, are mathematically equivalent. However, in contrast to adversarial examples, the change imposed in the counterfactual explanations are intended to be humanly understandable. Mathematically, we formalize this intuition as *fidelity* to the underlying data distribution: counterfactuals should have high fidelity, whereas adversarial examples have low fidelity. Adversarial examples can fool a classifier precisely because they are outside the data distribution, even though they look indistinguishable to training data samples for human observers. Fidelity, we argue, is also what brings explanatory value to counterfactuals: only if the counterfactual is a realistic, high-fidelity sample can it explain a minimal, meaningful change to a human observer, whereas adversarial examples impose meaningless changes.

We note that fidelity is related to the term *plausibility* from the explainability literature, yet we will use fidelity in the following as a specific case of plausibility with respect to the underlying probability density. We purposefully use the term fidelity in this paper rather than realism to contrast in- and out- of distribution examples to examples simply looking realistic upon human visual inspection.

The considerations above lead us to introduce another novel type of example-based explanation - *affirmative examples*. These are new high-fidelity examples which are consistent with the original decision that shall, as the name suggests, re-affirm the user understanding of the algorithm decisions by re-introducing the critical features altered through the counterfactuals. Conceptually, they can be thought of as counterfactual examples to counterfactuals, see the right part of figure 1. This idea is similar to the pertinent positives and negatives explored in an alternative approach to explainability (Dhurandhar et al. 2018), however, our approach does not find features which would necessarily have to be absent but instead reaffirms which changes introduced in the generated explanations are truly class-discriminative.

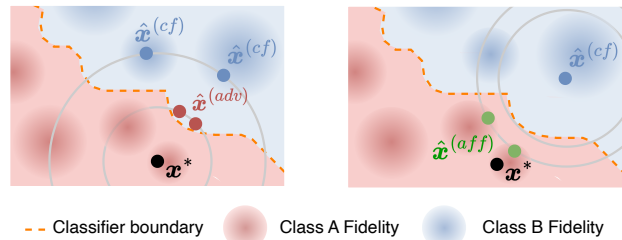


Figure 1: Schematic illustration of the relationships between local explanatory examples. *Left*: Original example \mathbf{x}^* has high-fidelity (comes from high-density area of the data distribution) and is classified as A. Adversarial examples $\hat{\mathbf{x}}^{(adv)}$ are low-fidelity samples (from a low-density area) near the original but classified as B. Counterfactuals $\hat{\mathbf{x}}^{(cf)}$ are also classified as B, but they are high-fidelity samples (high density area). They are close to the original sample but may be further away than the adversarial examples. *Right*: Affirmatives are high-fidelity samples classified as A near the counterfactual examples. In consequence, they come from high-density areas within A close to (though not necessarily coinciding with) \mathbf{x}^* .

We formalize the concepts of *counterfactual*, *affirmative* and *adversarial examples* introduced above within a new probabilistic framework for local explanatory examples in the following subsection.

2.1 Probabilistic definitions for local explanatory examples

Let $\mathbf{x}^* \in \mathcal{X}$ be a random sample from the true underlying generating data distribution p_{data} with the original classifier label $y_o \in \mathcal{Y}$; $\hat{\mathbf{x}} \in \mathcal{X}$ a synthetically generated sample; $y_t \in \mathcal{Y}$ the target class label; $d : \mathcal{X} \times \mathcal{X} \rightarrow \mathbb{R}_+$ a suitable user-specified distance function (such as ℓ_1 , ℓ_2 or some suitable perception distance). We define the following concepts with respect to the probabilistic classification algorithm p_{cl} and the original example \mathbf{x}^* :

Definition 1 (Counterfactual explanation) We call a synthetic data sample $\hat{\mathbf{x}}$ with **all** the following characteristics a targeted counterfactual explanation with respect to some target $y_t \in \mathcal{Y}$ and some thresholds $\delta, \epsilon > 0$:

- $\hat{\mathbf{x}}$ is **close** to the original sample \mathbf{x}^*

$$d(\hat{\mathbf{x}}, \mathbf{x}^*) \leq \delta ; \quad (2)$$

- $\hat{\mathbf{x}}$ is **valid** w.r.t. the **target label** classification area
$$p_{\text{cl}}(Y = y_t | \mathbf{X} = \hat{\mathbf{x}}) > p_{\text{cl}}(Y = y_j | \mathbf{X} = \hat{\mathbf{x}}) \quad (3)$$
for all $j \neq t$;

- $\hat{\mathbf{x}}$ has **high fidelity** to the real data distribution (**is a realistic data example**)

$$p_{\text{data}}(\mathbf{X} = \hat{\mathbf{x}}) \geq \epsilon . \quad (4)$$

Definition 2 (Affirmative explanation) We call a synthetic data sample $\hat{\mathbf{x}}$ with **all** the following characteristics an affirmative of a counterfactual $\hat{\mathbf{x}}^{(cf)}$ with some thresholds $\delta, \epsilon > 0$:

- $\hat{\mathbf{x}}$ is **close** to the counterfactual explanation $\hat{\mathbf{x}}^{(cf)}$

$$d(\hat{\mathbf{x}}, \hat{\mathbf{x}}^{(cf)}) \leq \delta ; \quad (5)$$

- $\hat{\mathbf{x}}$ is **valid** w.r.t. the **original label** y_o classification area

$$p_{cl}(Y = y_o | \mathbf{X} = \hat{\mathbf{x}}) > p_{cl}(Y = y_j | \mathbf{X} = \hat{\mathbf{x}}) \quad (6)$$

for all $j \neq o$;

- $\hat{\mathbf{x}}$ has **high fidelity** to the real data distribution (**is a realistic data example**)

$$p_{data}(\mathbf{X} = \hat{\mathbf{x}}) \geq \epsilon . \quad (7)$$

Definition 3 (Adversarial example) We call a synthetic data sample $\hat{\mathbf{x}}$ with **all** the following characteristics a targeted adversarial example with respect to some target $y_t \in \mathcal{Y}$ and some thresholds $\delta, \epsilon > 0$:

- $\hat{\mathbf{x}}$ is **close** to the original sample \mathbf{x}^*

$$d(\hat{\mathbf{x}}, \mathbf{x}^*) \leq \delta ; \quad (8)$$

- $\hat{\mathbf{x}}$ is **valid** w.r.t. the **target label** classification area

$$p_{cl}(Y = y_t | \mathbf{X} = \hat{\mathbf{x}}) > p_{cl}(Y = y_j | \mathbf{X} = \hat{\mathbf{x}}) \quad (9)$$

for all $j \neq t$;

- $\hat{\mathbf{x}}$ has **low fidelity** to the real data distribution (**is not a realistic data example**)

$$p_{data}(\mathbf{X} = \hat{\mathbf{x}}) \leq \epsilon . \quad (10)$$

We point out that the only difference in the definitions of adversarial and counterfactual examples is the fidelity criterion which shall be high for counterfactuals and low for adversarial examples.

It is important to note that all the above concepts are **local** (i.e., pertaining to the specific original sample \mathbf{x}^*) and **classifier-specific**. Furthermore, we can bring the above definitions into a fully probabilistic setting by reformulating the closeness constraints in the form of a prior distribution $p(\hat{\mathbf{x}}|\mathbf{x}^*)$ on the data sample $\hat{\mathbf{x}}$ (e.g., Gaussian for the ℓ_2 or Laplace for the ℓ_1 distances).

2.2 The generative explainer problem

Following the definitions in section 2.1, we formulate the search for explanatory examples as an optimization problem. We give it for the case of counterfactual examples; affirmatives and adversarial examples follow trivially in analogy.

$$\arg \max_{\hat{\mathbf{x}}} p_{cl}(Y = y_t | \mathbf{X} = \hat{\mathbf{x}}) \quad (\text{validity})$$

$$\text{s.t. } p_{data}(\mathbf{X} = \hat{\mathbf{x}}) \geq \epsilon, \quad (\text{fidelity})$$

$$d(\hat{\mathbf{x}}, \mathbf{x}^*) \leq \delta \quad (\text{closeness})$$

In practice, we typically have no access to the true underlying data distribution p_{data} other than through the observed data and therefore cannot evaluate the fidelity of the point $\hat{\mathbf{x}}$. We propose to replace the unknown true distribution by an approximation $p_{gen} \approx p_{data}$ learned by a suitable generative algorithm, enabling us to sample high fidelity examples $\hat{\mathbf{x}} \sim p_{gen}$. Our final formulation of the *generative explanation problem* reformulates the optimization into a Lagrangian form and subsumes the fidelity constraint into the sampling procedure:

$$\arg \max_{\hat{\mathbf{x}} \sim p_{gen}} \lambda p_{cl}(Y = y_t | \mathbf{X} = \hat{\mathbf{x}}) - d(\hat{\mathbf{x}}, \mathbf{x}^*) . \quad (11)$$

Though building up from our probabilistic definitions, this problem is consistent with the well established counterfactual explanation problem (1) of Wachter, Mittelstadt, and Russell (2017) with the additional fidelity constraint ensured implicitly through sampling from p_{gen} , thus linking the generative approach to local explainability akin to traditional approaches.

The particular choice of the hyperparameter λ , as well as the distance function, depends on one hand on the properties of the data and the decision algorithm, and on the other hand on user preferences and interests. For example, setting the hyperparameter λ to a higher value will favor examples further away from the original data point with higher confidence of the classifier. Explanatory examples generated under various settings of these values may provide the user with further valuable information about the decisions of the algorithm in the vicinity of the original sample through more diversity.

2.3 Evaluation of explanatory examples

The evaluation of explanatory algorithms and the quality of the explanatory examples remains a challenge (Väth et al. 2023). Though human studies based on visual inspection are expected to provide valuable feedback, they are challenging to undertake and often suffer from a number of deficiencies introduced due to practical considerations (e.g., expertise mismatch, motivation bias, experience learning curve, time constraints, etc. (Lage et al. 2019; Rosenfeld 2021)). To avoid these, we propose a quantitative evaluation scheme for explanatory examples following the three characteristics discussed in section 2.1: closeness, validity, and fidelity.

We propose to measure *closeness* of the explanatory examples by their distance to the original sample. Commonly used metrics include the ℓ_p distances, for example the ℓ_1 -distance for sparser changes or the ℓ_2 -distance for broader changes across the input. The distance metric should be coherent with the one used in the generative algorithm formulation in equation (11).

For *validity*, we propose to report the classifier prediction confidence for the target class. We acknowledge that the output of the neural network classifier is not a reliable indicator for the classifier confidence (Hein, Andriushchenko, and Bitterwolf 2019). Nevertheless, we consider it a good-enough measure when comparing a single algorithm across multiple explanatory examples.

For *fidelity*, it is common in the generative modeling community to use metrics based on distribution matching (e.g., Fréchet inception distance (FID) (Heusel et al. 2017), Inception Score (IS) (Salimans et al. 2016) or Precision/Recall (Sajjadi et al. 2018)); however, these measures are not suitable for evaluating individual examples. Instead, we propose to directly use the negative log-likelihood (NLL) of the generated example (Artelt and Hammer 2020) in comparison to the NLL of the original example. An explanatory example should have a similar NLL as the original, whereas an adversarial should have a relatively lower NLL.

In addition to evaluating the algorithm, we can provide the metrics as complementary information to the user. We recommend that the user generates multiple explanatory ex-

amples possibly with variations in the thresholds and hyperparameters for the generative explanatory problem (section 2.2). The metrics vary according to the diversity of the generated examples and thus can further reinforce the user understanding of the classifier decision (discussion of table 5).

3 Diffusion-generated explanatory examples

In this section, we showcase the use of the framework in a constructive manner when developing new algorithms for generative local explanations. As a baseline, we develop an algorithm based on the *generative explanation problem* (11) introduced in section 2. We choose to work with Denoising Diffusion Probabilistic Models (DDPM) (Ho, Jain, and Abbeel 2020; Dhariwal and Nichol 2021; Song et al. 2021) as the generative model p_{gen} for sampling **high fidelity** examples and leverage the capabilities of classifier guidance to steer the generations towards desirable output in terms of their **validity** and **closeness** according to our definitions in section 2.1.

3.1 DDPM preliminaries

DDPMs are latent variable models that are trained to approximate the underlying data distribution p_{data} via a model $p_{\theta}(\mathbf{x}_0) = \int p_{\theta}(\mathbf{x}_0|\mathbf{x}_1) \prod_{t=1}^T p_{\theta}(\mathbf{x}_{t-1}|\mathbf{x}_t) d\mathbf{x}_{1:T}$. They follow an encoder-decoder architecture: the encoder (forward process) is defined as a Markov chain Gaussian model $q(\mathbf{x}_t|\mathbf{x}_{t-1}) := \mathcal{N}(\mathbf{x}_t; \sqrt{1-\beta_t}\mathbf{x}_{t-1}, \beta_t\mathbf{I})$, progressively adding random Gaussian noise to an original example \mathbf{x}_0 with a pre-defined variance schedule β_1, \dots, β_T over the diffusion steps $\mathbf{x}_1, \dots, \mathbf{x}_T$ so that $\mathbf{x}_T \sim \mathcal{N}(0, \mathbf{I})$; the Gaussian Markov decoder (reverse process) $p_{\theta}(\mathbf{x}_{t-1}|\mathbf{x}_t)$ learns to revert the forward diffusion process (encoder) by gradually removing noise from the signal \mathbf{x}_t to produce samples matching the original data distribution $p_{\theta} \approx p_{\text{data}}$.

Instead of maximizing the intractable likelihood p_{θ} , DDPMs can be trained by a simplified objective that matches the noise predicted by the denoising reverse process $\hat{\epsilon}_{\theta}(\mathbf{x}_t, t)$ to the ground truth noise ϵ^* of the forward process.

$$L_{\text{simple}} := \mathbb{E}_{\mathbf{x}_t \sim \mathcal{U}(1, T), \mathbf{x}_0 \sim q(\mathbf{x}_0), \epsilon^* \sim \mathcal{N}(0, \mathbf{I})} \|\epsilon^* - \hat{\epsilon}_{\theta}(\mathbf{x}_t, t)\|^2, \quad \text{where } \mathbf{x}_t = \sqrt{\bar{\alpha}_t} \mathbf{x}_0 + \epsilon^* \sqrt{1 - \bar{\alpha}_t},$$

which is a simplified, reweighted version of the tractable evidence lower bound (ELBO), with $\bar{\alpha}_t = \prod_{s=1}^t (1 - \beta_s)$.

$$\begin{aligned} \log p_{\theta}(\mathbf{x}_0) &\geq \underbrace{\mathbb{E}_q[\log p_{\theta}(\mathbf{x}_0|\mathbf{x}_1)]}_{\text{reconstruction term}} \\ &\quad - \underbrace{D_{\text{KL}}(q(\mathbf{x}_T|\mathbf{x}_0) \| p(\mathbf{x}_T))}_{\text{prior matching term}} \\ &\quad - \sum_{t=2}^T \underbrace{\mathbb{E}_q[D_{\text{KL}}(q(\mathbf{x}_{t-1}|\mathbf{x}_t, \mathbf{x}_0) \| p_{\theta}(\mathbf{x}_{t-1}|\mathbf{x}_t))]}_{\text{denoising matching term}} \end{aligned}$$

3.2 Classifier guidance

The vanilla DDPM introduced in section 3.1 enables synthesizing random samples $\hat{\mathbf{x}} \sim p_{\theta} \approx p_{\text{data}}$ with high

fidelity to the underlying data distribution. However, to generate valid class-specific data points such as counterfactual explanations, the reverse process has to be conditioned on the target label $p_{\theta}(\mathbf{x}_{t-1}|\mathbf{x}_t, y)$. For an unconditionally trained (label-unaware) DDPM $p_{\theta}(\mathbf{x}_{t-1}|\mathbf{x}_t) = \mathcal{N}(\mathbf{x}_{t-1}; \mu_t(\mathbf{x}_t), \Sigma_t(\mathbf{x}_t))$, the mean μ_t of the denoising transition can be shifted by the gradients of a classifier $\nabla_{\mathbf{x}_t} \log p_{\text{cl}}(y|\mathbf{x}_t)$ trained over the noisy data \mathbf{x}_t to yield class-conditional samples as follows (Sohl-Dickstein et al. 2015; Dhariwal and Nichol 2021):

$$\mu'_t = \mu_t + s \Sigma_t \nabla_{\mathbf{x}_t} \log p_{\text{cl}}(y|\mathbf{x}_t), \quad (12)$$

where s is a gradient scaling factor controlling the strength of the classifier guidance.

3.3 Classifier guidance for explanatory examples

The mechanism for classifier guidance outlined in section 3.2 opens a window of opportunity for generating explanatory examples coherent with our definitions in section 2.1. However, there are two important points that remain to be addressed. The first is the requirement for closeness - the generated counterfactual examples shall be close to the original data $d(\mathbf{x}^*, \hat{\mathbf{x}}^{(cf)}) \leq \delta$. The second is related to the training data of the decision algorithm being explained - the classifier guidance mechanism requires the classifier to be trained on the noisy data of the DDPM. This is, however, unattainable within the explainability context where we aim to explain the decisions of an independently trained classifier.

In our algorithm for diffusion-generated explanatory examples (**XAIDIFF**), we build on the previous work for diffusion-based counterfactuals (Augustin et al. (2022); Jeanneret, Simon, and Jurie (2022)), but propose several improvements motivated by our definitions in section 2.1. Similarly to Augustin et al. (2022), we use the quick denoised predictions to obtain the classifier gradients $\nabla_{\mathbf{x}_t} \log p_{\text{cl}}(y|\hat{\mathbf{x}}_0^{(x_t)})$ and to ensure the closeness to the original data example through an ℓ_1 distance. Concretely, we formulate the guidance step as follows:

$$\begin{aligned} \mu'_t &= \mu_t + \Sigma_t \nu(g, t), \\ g &= \nabla_{\mathbf{x}_t} \left[\lambda \log p_{\text{cl}}(y|\hat{\mathbf{x}}_0^{(x_t)}) - \|\hat{\mathbf{x}}_0^{(x_t)} - \mathbf{x}^*\|_1 \right]. \quad (13) \end{aligned}$$

However, we do not truncate the diffusion but start from random white noise $\mathbf{x}_T \sim \mathcal{N}(\mathbf{0}, \mathbf{I})$. This leads to a less constrained search space and allows for higher fidelity and diversity in the generated explanatory examples.

Instead of relying on a surrogate robust classifier as in Augustin et al. (2022), we tackle the problem of gradient instability head-on (Vaeth et al. 2024). We interpret the gradient guidance in equation (13) as stochastic gradient descent steps of the mean μ_t of the denoising transitions towards maximum of the classifier p_{cl} and minimum distance d . Motivated by this view, we propose to leverage modern methods for stochastic optimization of non-stationary objectives with noisy gradients. Concretely, we introduce ADAM (Kingma and Ba 2017) into the guidance steps (function $\nu(\cdot)$ in equation (13)) to automatically adapt the learning rates from estimates of the first and second moments of the gradients.

Finally, we link the guidance steps back to our initial definitions of explanatory examples from section 2. We can interpret the individual terms as gradients of the *generative explanation problem* (11) introduced in section 2.2:

- μ_θ implicitly as the gradient towards maximum fidelity,
- $\nabla_{\mathbf{x}_t} [\log p_{\text{cl}}(y | \hat{\mathbf{x}}_0^{(x_t)})]$ as the gradient towards maximum classifier validity, and
- $\nabla_{\mathbf{x}_t} [\|\hat{\mathbf{x}}_0^{(x_t)} - \mathbf{x}^*\|_1]$ as the gradient to maximum closeness to the original sample.

4 Experiments

In this section, we put our algorithm XAIDIFF into use, demonstrate its ability to generate explanatory examples and discuss practical aspects of the definitions in section 2.1. The aim of this section is to showcase our probabilistic framework in a constructive manner through XAIDIFF and provide a currently lacking baseline for future development.

4.1 Datasets & Experimental Setup

We provide experimental results on two main data sets. The first is a newly proposed synthetic data set, named SportBalls, carefully designed to provide a simple and controlled explanation scenario where the optimal explanation is intuitively clear. We then perform a more comprehensive set of experiments on the real-world data set CelebA (Liu et al. 2015). We show results for one more data set (MNIST (LeCun et al. 1998)) in the appendix.

SportBalls The custom data set is created by randomly selecting three out of five sport balls and placing them at random coordinates on white background with random rotation and scaling. There can be multiple types of sport balls in one image and the balls may overlap (even occlude each other), creating a more complex yet controlled explanation setting. The data set is carefully created to have similar objects (i.e., scaling, shape, size, rotation and placement) but with clear semantic differences (i.e., colors and pattern). We use this new data set to illustrate key components of our framework. The data set and code are provided in the supplementary material for further re-use by the community.

For the experiments on the SportBalls data, we picked four starting images each containing at least one soccer ball with varying complexity for the explanation: first image where the sport balls are non-overlapping, the second image with multiple soccer balls, the third image where the soccer ball is the background of another sport ball, and the fourth image where the soccer ball is partly occluded.

CelebA As the real-world data set, we use CelebA (Liu et al. 2015) (downscaled to 64x64) for both the classifier and the DDPM. CelebA is a publicly available data set of celebrity faces with easily recognizable attributes that serve as targets for the classification task. As starting points for explanations on CelebA, we picked four images of faces with negative values for all three attributes: no eyeglasses, no smile, not blond. The selection was done before exposing the examples to any of the algorithms based purely on

their diversity in terms of gender, hairstyle, formal attire and background, to support analysis of the outcomes under varied settings.

Classifiers & DDPM In a realistic explainability scenario, the classifier to be explained is provided externally. In our experiments we therefore pick a standard architecture for the classifiers, a low-resource small version of the MobileNetV3 (Howard et al. 2019) from ‘torchvision’, and train a classifier to recognize soccer balls in the Sportballs dataset to an 96.8 % test accuracy, and a multi-label classifier for CelebA, recognizing three binary attributes - the presence or absence of eyeglasses, smile, and blond hair - to 97.13%, 89.71% and 93.33% test accuracy. Our XAIDIFF algorithm assumes access to a DDPM trained over the same data distribution as the classifier. We therefore train the DDPM for the XAIDIFF algorithm over the same data sets. The implementation relies on the open-source Diffusers toolbox (von Platen et al. 2022).

Evaluation We evaluate closeness, validity and fidelity of the XAIDIFF generations according to our proposed evaluation schema in section 2.3. We measure *closeness* of the explanatory examples by their ℓ_1 -distance to the original sample. The distance metric is coherent with the one used in our XAIDIFF algorithm formulation in equation (13). For *validity*, we report the classifier prediction confidence for the target class. Finally, we can approximate the negative log-likelihood (NLL) by evaluating the variational lower bound (ELBO) of the learned model p_θ as the measure of *fidelity*.

We employ the above metrics to document the correct functioning of the XAIDIFF algorithm. For this, we compare the averages of the metrics across a set of examples generated by the algorithm for the different categories of explanatory examples. For instance, a well functioning algorithm shall ensure that counterfactual examples have on average higher fidelity than adversarial examples.

4.2 Generative explanatory examples

In this section, we validate that XAIDIFF produces valid counterfactual explanations whereas adversarial examples and other ablations fail, empirically showing that all three criteria from section 2.1. - validity, closeness, fidelity, are necessary and need to be explicitly enforced in the algorithm to achieve valid counterfactuals.

We show one XAIDIFF generation per starting image of both data sets in table 6 and the corresponding metrics in table 2. More generations are shown in the appendix. For the SportBalls data set, the counterfactual explanations should show how the image needs to change for the classifier to decide there are no soccer balls. The starting images \mathbf{x}^* are correctly classified as soccerball=yes (indicated by a blue stripe on top of the images). For the CelebA data set, it is the binary attribute eyeglasses=no, which shall be changed to yes for the explanation.

We discuss the results of tables 6 and 2 for the synthetic SportBalls data set in detail. Our findings follow in analogy for the real-world CelebA data set shown the lower part of the tables.

The counterfactual explanations in table 6 (second column), resulting from the XAIDIFF algorithm, are all valid according to the classifier (no soccer ball) - indicated by a green stripe on top of the images - and close to the original image, but not as close as $\hat{x}^{(adv)}$ - indicated quantitatively by the ℓ_1 -distance (table 2). The adversarial examples ($\hat{x}^{(adv)}$), generated through simple gradient updates $\hat{x} \leftarrow \hat{x} + \nabla_{\hat{x}} p_{cl}(y_t | \hat{x})$ within the pixel space towards the classification target, are valid but do not show semantical change (i.e., the soccer ball is still clearly visible). The visual inspection is confirmed by high bits-per-dim values in table 2 indicating the adversarial examples are relatively low-fidelity generations, providing little explanatory value.

The fourth column ($\hat{x}^{(cf \setminus c)}$) in table 6 removes the *closeness* criterion. Accordingly, this ablation produces samples which are still valid (the classifier predicts no soccer balls) and high-fidelity (there are in fact no visible soccer balls) but distant - i.e. the example has no visible connection to the original sample anymore, making it useless as an explanatory example. The last column ($\hat{x}^{(cf \setminus v)}$) in table 6 removes the *validity* criterion. With this factor removed, XAIDIFF generates high-fidelity examples very close the original examples without changing the decision of the classifier and hence not helping to explain the classifier decisions.

	x^*	$\hat{x}^{(cf)}$	$\hat{x}^{(adv)}$	$\hat{x}^{(cf \setminus c)}$	$\hat{x}^{(cf \setminus v)}$
SportBalls					
CelebA					

Table 1: Original SportBalls/CelebA examples x^* compared to counterfactuals $\hat{x}^{(cf)}$, adversarial examples $\hat{x}^{(adv)}$, and XAIDIFF generations without closeness $\hat{x}^{(cf \setminus c)}$ and validity criteria $\hat{x}^{(cf \setminus v)}$, respectively. The original images are classified as false for the attributes soccerball/eyeglasses.

	x^*	$\hat{x}^{(cf)}$	$\hat{x}^{(adv)}$	$\hat{x}^{(cf \setminus c)}$	$\hat{x}^{(cf \setminus v)}$	
SportBalls	c_{\downarrow}	-	0.7 (0.3)	0.0 (0.0)	1.2 (0.3)	0.1 (0.1)
	v_{\uparrow}	-	100 (0.0)	83.4 (29.6)	100 (0.0)	51.5 (44.2)
	f_{\downarrow}	0.3	0.6 (0.4)	0.7 (0.1)	0.9 (0.4)	0.3 (0.1)
CelebA	c_{\downarrow}	-	0.6 (0.1)	0.1 (0.0)	4.7 (0.7)	0.6 (0.1)
	v_{\uparrow}	-	99.5 (0.3)	86.5 (20.7)	99.3 (0.8)	0.5 (0.5)
	f_{\downarrow}	2.9	2.5 (0.2)	4.0 (0.4)	3.1 (0.4)	2.4 (0.2)

Table 2: Evaluation metrics for SportBalls/CelebA counterfactual explanations and ablations with the single-class soccerball/eyeglasses attribute (false \rightarrow true): closeness as ℓ_1 -distance per dim, validity in % of classifier confidence, fidelity as negative ELBO in bits-per-dim.

	x^*	$\hat{x}^{(cf)}$	$\hat{x}^{(aff)}$	x^*	$\hat{x}^{(cf)}$	$\hat{x}^{(aff)}$
Single-label						
Multi-label						

Table 3: Original examples x^* compared to counterfactuals $\hat{x}^{(cf)}$ and affirmatives $\hat{x}^{(aff)}$. Single-label for eyeglasses false \rightarrow true; multi-label for eyeglasses false \rightarrow true and smiling false \rightarrow true and blond false \rightarrow true. More generations per starting image in the appendix.

	metrics	x^*	$\hat{x}^{(cf)}$	$\hat{x}^{(aff)}$
Single-label	$c_{\downarrow}(x^*)$	-	0.6 (0.1)	0.6 (0.1)
	$c_{\downarrow}(\hat{x}^{(cf)})$	-	-	0.2 (0.1)
	v_{\uparrow}	-	99.5 (0.3)	99.5 (0.4)
	f_{\downarrow}	2.6 (0.2)	2.5 (0.2)	2.5 (0.2)
Multi-label	$c_{\downarrow}(x^*)$	-	0.57 (0.12)	0.64 (0.15)
	$c_{\downarrow}(\hat{x}^{(cf)})$	-	-	0.24 (0.04)
	v_{\uparrow}	-	89.17 (4.95)	97.24 (1.13)
	f_{\downarrow}	2.85 (0.28)	2.58 (0.18)	2.60 (0.23)

Table 4: Evaluation metrics for explanatory examples - affirmatives: closeness as ℓ_1 -distance per dim, validity in % of classifier confidence, fidelity as negative ELBO in bits-per-dim. Single-label for eyeglasses false \rightarrow true; multi-label for eyeglasses false \rightarrow true and smiling false \rightarrow true and blond false \rightarrow true.

In tables 9 and 4, we showcase the new type of explanatory examples - the affirmative explanations - using the CelebA data set. We contrast the affirmatives to the originals and the counterfactuals to demonstrate their explanatory value. As we see in the tables, the affirmatives are high-fidelity examples classified the same as the original examples (blue stripe) and they indeed do not contain the concepts introduced by the counterfactual explanations. Though being close to the originals, they are even closer to the counterfactuals (see closeness in table 4). These characteristics are in line with the definitions provided in section 2.1 and experimentally demonstrates the intuitions depicted in the schematic illustration in figure 1. From an explainability perspective, the affirmatives shall help the user re-affirm his understanding of the classifier decisions in terms of adding (counterfactuals) and removing (affirmatives) the class-discriminative concepts from the examples.

In the bottom of tables 9 and 4, we show that the findings above naturally extend also to more complex multi-label explanation scenarios: the counterfactuals and affirmatives generated by XAIDIFF correctly trigger changes in the classifier decisions, flipping the classifications for all three attributes together - from no in the original to yes in the counterfactuals and back to no in the affirmatives. All these changes are also corroborated by high validity values in table 4 and clearly observable in the generated images in table 9.

As explained in section 2.3, another benefit of the evaluation metrics is their explanatory value for the user. We illustrate this in table 5, where we supplement four counterfactual explanations with their respective metrics. The counterfactuals were generated with varying values of the validity-closeness trade-off hyperparameter λ in equation (13). Referring to the metric values, the user can better appreciate the difference between the counterfactual examples, which in turn shall help to explain the classifier decision. For instance, the validity of the first counterfactual in table 5 is lower than of the other three examples which corresponds to smaller recognizability of the eyeglasses in the image. Giving the responsibility of selecting a good explanation to the user with very individual preferences may be an interesting direction for future work.

x^*	$\hat{x}_{0.1}^{(cf)}$	$\hat{x}_{0.3}^{(cf)}$	$\hat{x}_{0.5}^{(cf)}$	$\hat{x}_{0.7}^{(cf)}$
				
c_{\downarrow}	0.37	0.37	0.49	0.50
v_{\uparrow}	96.23	98.91	99.92	99.74
f_{\downarrow}	2.29	2.33	2.34	2.29

Table 5: Metrics as supplementary explanatory information - validity-closeness trade-off $\lambda \in \{0.1, 0.3, 0.5, 0.7\}$

5 Conclusion

Recent methods for generative example-based explanations show impressive sample quality outlining a promising direction for future research. However, the papers presenting these methods (Augustin et al. 2022; Jeanneret, Simon, and Jurie 2022) are unfortunately largely inconsistent in used definitions, experimental baselines and approaches to evaluation. They are also rather disconnected from previous work on machine learning explainability (e.g., on tabular data) often disregarding basic assumptions and expectations of the field. This disconnect between the generative modeling and explainability communities leads to many misunderstandings which may transform to idle dismissive attitudes and in effect hinder scientific development. To bridge this gap, this paper puts forward a novel probabilistic framework for local explanatory examples consistent with traditional explainability desiderata and demonstrates how it can be used constructively for developing new generative-based explanatory algorithms by proposing the diffusion-based XAIDIFF algorithm. The framework defines counterfactual explanations as high-fidelity, valid and close examples, contrasts these to low-fidelity adversarial examples and introduces affirmative examples as a novel type of example-based explanations. To evaluate explanatory examples, the framework includes a quantitative evaluation schema coherent with the definitions, providing a measurable alternative to the often subjective visual inspection prevalent in the field. To support development of future example-based algorithms, we propose and release a new synthetic SportBalls data set as a controlled environment for explainability in the high-dimensional setting. The application of the XAIDIFF algorithm for explaining classifier decisions on the SportsBall and CelebA image data sets illustrates the potential of the framework for improving the user understanding and trust in classifier decisions as well as for future algorithmic developments. In line with the best research practice, we foster transparency and reproducibility by providing the complete implementation of our method together with the full settings to reproduce the results of our experiments in the supplementary material.

Limitations Individual users may react to explanations differently depending on their own experience or personal affinity. Our algorithm is not able to adapt to such user variations. The metrics we propose are derived from our definitions and do not measure the appropriateness of the examples for improved user understanding. Our method assumes the availability of a diffusion model trained over the same (or sufficiently similar) data as the classifier. This may be impossible in practice. There are also no mathematical guarantees for the proposed method.

Ethical Statement As any other generative model, our method could be used to produce malicious content. This would, however, require access to a white-box classifier trained over malicious attributes which reduces the risk of misuse. On the other hand, our method could foster transparency and acceptance of AI models through improved explainability and prevent erroneous decisions through better understanding of classification decisions.

6 Acknowledgments

This work was supported by the Bavarian HighTech agenda and the Wuerzburg Center for Artificial Intelligence (CAIRO) of the Technical University of Applied Sciences Wuerzburg-Schweinfurt (THWS).

References

- Adadi, A.; and Berrada, M. 2018. Peeking inside the black-box: a survey on explainable artificial intelligence (XAI). *IEEE access*, 6: 52138–52160.
- Artelt, A.; and Hammer, B. 2020. Convex density constraints for computing plausible counterfactual explanations. In *Artificial Neural Networks and Machine Learning—ICANN 2020: 29th International Conference on Artificial Neural Networks, Bratislava, Slovakia, September 15–18, 2020, Proceedings, Part I* 29, 353–365. Springer.
- Augustin, M.; Boreiko, V.; Croce, F.; and Hein, M. 2022. Diffusion visual counterfactual explanations. *Advances in Neural Information Processing Systems*, 35: 364–377.
- Chatila, R.; Dignum, V.; Fisher, M.; Giannotti, F.; Morik, K.; Russell, S.; and Yeung, K. 2021. Trustworthy ai. *Reflections on Artificial Intelligence for Humanity*, 13–39.
- Das, A.; and Rad, P. 2020. Opportunities and Challenges in Explainable Artificial Intelligence (XAI): A Survey. arXiv:2006.11371.
- Delaney, E.; Greene, D.; and Keane, M. T. 2021. Uncertainty Estimation and Out-of-Distribution Detection for Counterfactual Explanations: Pitfalls and Solutions. arXiv:2107.09734.
- Dhariwal, P.; and Nichol, A. 2021. Diffusion models beat gans on image synthesis. *NeurIPS*, 34: 8780–8794.
- Dhurandhar, A.; Chen, P.-Y.; Luss, R.; Tu, C.-C.; Ting, P.; Shanmugam, K.; and Das, P. 2018. Explanations based on the missing: Towards contrastive explanations with pertinent negatives. *Advances in neural information processing systems*, 31.
- Goodfellow, I. J.; Shlens, J.; and Szegedy, C. 2015. Explaining and Harnessing Adversarial Examples. arXiv:1412.6572.
- Goodman, B.; and Flaxman, S. 2017. European Union regulations on algorithmic decision-making and a “right to explanation”. *AI magazine*, 38(3): 50–57.
- Guidotti, R. 2022. Counterfactual explanations and how to find them: literature review and benchmarking. *Data Mining and Knowledge Discovery*, 1–55.
- Gunning, D. 2017. Explainable artificial intelligence (xai). *Defense advanced research projects agency (DARPA), nd Web*, 2(2): 1.
- Hein, M.; Andriushchenko, M.; and Bitterwolf, J. 2019. Why relu networks yield high-confidence predictions far away from the training data and how to mitigate the problem. In *Proceedings of the IEEE/CVF Conference on Computer Vision and Pattern Recognition*, 41–50.
- Heusel, M.; Ramsauer, H.; Unterthiner, T.; Nessler, B.; and Hochreiter, S. 2017. GANs trained by a two time-scale update rule converge to a local nash equilibrium. In *Proceedings of the 31st International Conference on Neural Information Processing Systems, NIPS’17*, 6629–6640. Red Hook, NY, USA: Curran Associates Inc. ISBN 9781510860964.
- Ho, J.; Jain, A.; and Abbeel, P. 2020. Denoising diffusion probabilistic models. *NeurIPS*, 33: 6840–6851.
- Howard, A.; Sandler, M.; Chu, G.; Chen, L.-C.; Chen, B.; Tan, M.; Wang, W.; Zhu, Y.; Pang, R.; Vasudevan, V.; et al. 2019. Searching for mobilenetv3. In *Proceedings of the IEEE/CVF International Conference on Computer Vision*, 1314–1324.
- Jeanneret, G.; Simon, L.; and Jurie, F. 2022. Diffusion models for counterfactual explanations. In *Proceedings of the Asian Conference on Computer Vision*, 858–876.
- Kingma, D. P.; and Ba, J. 2017. Adam: A Method for Stochastic Optimization. arXiv:1412.6980.
- Lage, I.; Chen, E.; He, J.; Narayanan, M.; Kim, B.; Gershman, S.; and Doshi-Velez, F. 2019. An Evaluation of the Human-Interpretability of Explanation. arXiv:1902.00006.
- LeCun, Y.; Bottou, L.; Bengio, Y.; and Haffner, P. 1998. Gradient-based learning applied to document recognition. *Proceedings of the IEEE*, 86(11): 2278–2324.
- Liu, Z.; Luo, P.; Wang, X.; and Tang, X. 2015. Deep Learning Face Attributes in the Wild. In *Proceedings of International Conference on Computer Vision (ICCV)*.
- Rosenfeld, A. 2021. Better metrics for evaluating explainable artificial intelligence. In *Proceedings of the 20th international conference on autonomous agents and multiagent systems*, 45–50.
- Sajjadi, M. S.; Bachem, O.; Lucic, M.; Bousquet, O.; and Gelly, S. 2018. Assessing generative models via precision and recall. *Advances in neural information processing systems*, 31.
- Salimans, T.; Goodfellow, I.; Zaremba, W.; Cheung, V.; Radford, A.; and Chen, X. 2016. Improved Techniques for Training GANs. arXiv:1606.03498.
- Sohl-Dickstein, J.; Weiss, E.; Maheswaranathan, N.; and Ganguli, S. 2015. Deep unsupervised learning using nonequilibrium thermodynamics. In *International conference on machine learning*, 2256–2265. PMLR.
- Song, Y.; Sohl-Dickstein, J.; Kingma, D. P.; Kumar, A.; Ermon, S.; and Poole, B. 2021. Score-Based Generative Modeling through Stochastic Differential Equations. arXiv:2011.13456.
- Vaeth, P.; Fruehwald, A. M.; Paassen, B.; and Gregorova, M. 2024. GradCheck: Analyzing classifier guidance gradients for conditional diffusion sampling. arXiv:2406.17399.
- Väth, P.; Fruehwald, A. M.; Paaßen, B.; and Gregorova, M. 2023. Diffusion-based Visual Counterfactual Explanations - Towards Systematic Quantitative Evaluation. *eXplainable Knowledge Discovery in Data Mining (XKDD) workshop at ECML PKDD*.
- Verma, S.; Boonsanong, V.; Hoang, M.; Hines, K. E.; Dickerson, J. P.; and Shah, C. 2022. Counterfactual Explanations and Algorithmic Recourses for Machine Learning: A Review. arXiv:2010.10596.

von Platen, P.; Patil, S.; Lozhkov, A.; Cuenca, P.; Lambert, N.; Rasul, K.; Davaadorj, M.; and Wolf, T. 2022. Diffusers: State-of-the-art diffusion models. <https://github.com/huggingface/diffusers>.

Wachter, S.; Mittelstadt, B.; and Russell, C. 2017. Counterfactual explanations without opening the black box: Automated decisions and the GDPR. *Harv. JL & Tech.*, 31: 841.

A Technical Appendix

Generative Example-Based Explanations: Bridging the Gap between Generative Modeling and Explainability

A.1 SportBalls data set

The SportBalls data set (3x128x128) is synthetically created by randomly selecting three out of five sport balls and placing them at random coordinates on white background with random rotation and random scaling. It is possible to have more than one type of sport ball in one image and the balls may overlap (even occlude each other). The data set is created to have similar objects (i.e., scaling, shape, size, rotation and placement) but with clear semantic differences (i.e., the color and the pattern of the sport balls). The images used in the data set are by Freepik (<https://www.flaticon.com/authors/freepik>).

We train a MobileNetV3 binary classifier (about 1.5M parameters) on soccerball=yes/no for 10 epochs on a single Nvidia A100 80 GB GPU (about 3 minutes). The final test accuracy is 96.8 %. We train a DDPM model (about 22.5M parameters) for 1000 epochs on a single Nvidia A100 80 GB GPU (1 day 18 hours). The models are trained with the standard Diffusers training script provided in our code base. There was no early stopping or more advanced training schemas involved. We provide more generations for other starting images in table 6, complementing table 1 in the main paper.

A.2 CelebA data set

We trained our diffusion model on CelebA (3x64x64) for 1000 epochs, about 4 days, on a single NVIDIA A100 80 GB GPU. In the sections below, we provide additional experiments on the CelebA data. We provide more generations for other starting images in table 8 with the corresponding metrics in table 7, complementing table 1 in the main paper.

A.3 Multiple generations

We provide additional generations for the four original starting images to complement tables 1 and 3 in the main paper, see table 9.

A.4 Different classes

To extend our experiments to other classes, we show additional samples on the classes blond (table 10) and smiling (table 11), with the metrics directly included in the tables.

A.5 Different starting images

The starting images in the main paper were picked based on diversity. To illustrate the method on truly random images, we show samples on the first 16 images of the CelebA train set on the eyeglasses attribute in the following table 12 and the corresponding metrics in table 13.

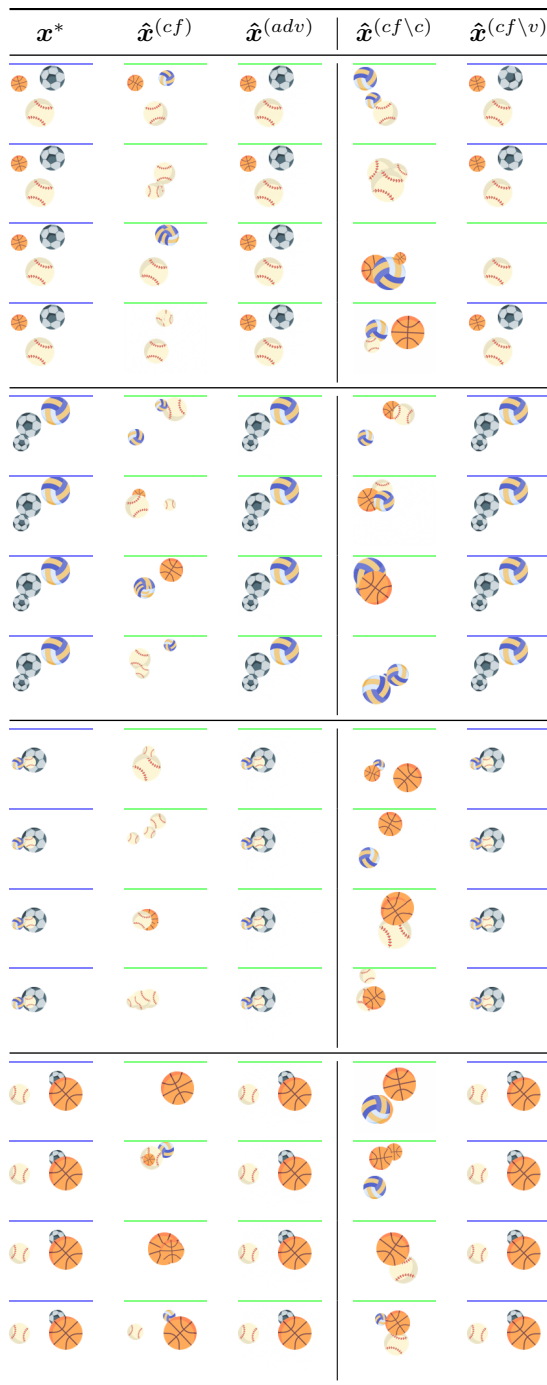


Table 6: Original SportBalls examples x^* compared to counterfactuals $\hat{x}^{(cf)}$, adversarial examples $\hat{x}^{(adv)}$, and XAID-IFF generations with closeness $\hat{x}^{(cf\setminus c)}$ and validity factors $\hat{x}^{(cf\setminus v)}$ disabled.

	\mathbf{x}^*	$\hat{\mathbf{x}}^{(cf)}$	$\hat{\mathbf{x}}^{(adv)}$	$\hat{\mathbf{x}}^{(cf \setminus c)}$	$\hat{\mathbf{x}}^{(cf \setminus v)}$
\mathbf{c}_\downarrow	-	0.56 (0.1)	0.06 (0.0)	4.74 (0.7)	0.56 (0.1)
\mathbf{v}_\uparrow	-	99.48 (0.3)	86.50 (20.7)	99.29 (0.8)	0.53 (0.5)
\mathbf{f}_\downarrow	2.85	2.50 (0.2)	3.95 (0.4)	3.06 (0.4)	2.44 (0.2)

Table 7: Evaluation metrics for explanatory examples - counterfactuals: **c**loseness as ℓ_1 -distance per dim in pixel values, **v**alidity in % of classifier confidence, **f**idelity as negative ELBO in bits-per-dim.

A.6 Different data set

In this section, we provide additional visual examples and respective metrics on MNIST, as a conceptually different data set than CelebA. For MNIST (1x16x16), the DDPM training time was around 2.5 hours for 100 epochs on the same setup as above. The results in table 14 (images) and table 15 (metrics) reaffirm the findings presented in the main paper.

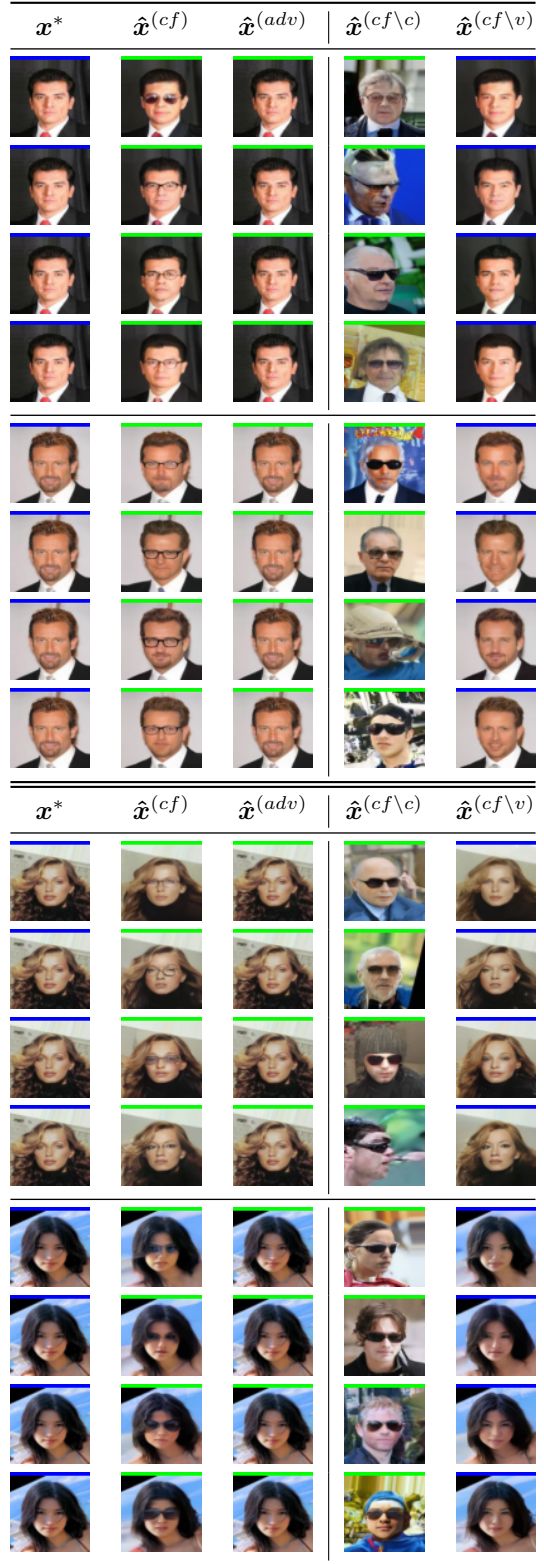


Table 8: Original examples \mathbf{x}^* compared to counterfactuals $\hat{\mathbf{x}}^{(cf)}$, adversarial examples $\hat{\mathbf{x}}^{(adv)}$ and XAIDIFF generations with closeness $\hat{\mathbf{x}}^{(cf \setminus c)}$ and validity factors $\hat{\mathbf{x}}^{(cf \setminus v)}$ disabled.

	x^*	$\hat{x}^{(cf)}$	$\hat{x}^{(aff)}$	x^*	$\hat{x}^{(cf)}$	$\hat{x}^{(aff)}$
Single-label: eyeglasses $X \rightarrow \checkmark$						
Multi-label: eyeglasses $X \rightarrow \checkmark$ and smiling $X \rightarrow \checkmark$ and blond $X \rightarrow \checkmark$						

Table 9: Original examples x^* compared to counterfactuals $\hat{x}^{(cf)}$ and affirmatives $\hat{x}^{(aff)}$. \times attribute classified as false; \checkmark as true

x^*	$\hat{x}^{(cf)}$	$\hat{x}^{(aff)}$	$\hat{x}^{(adv)}$	$\hat{x}^{(cf \setminus c)}$	$\hat{x}^{(cf \setminus v)}$
$c_{\downarrow}(x^*)$	0.6	0.7	0.0	4.6	0.4
$c_{\downarrow}(\hat{x}^{(cf)})$	-	0.2	0.6	4.5	
v_{\uparrow}	100	100	0	100	6
f_{\downarrow}	2.6	2.6	3.2	3.0	2.5

Table 10: CelebA class *blond* - Original examples x^* compared to counterfactuals $\hat{x}^{(cf)}$, adversarial examples $\hat{x}^{(adv)}$ and XAIDIFF generations with closeness $\hat{x}^{(cf \setminus c)}$ and validity factors $\hat{x}^{(cf \setminus v)}$ disabled. No standard deviation for brevity.

\mathbf{x}^*	$\hat{\mathbf{x}}^{(cf)}$	$\hat{\mathbf{x}}^{(aff)}$	$\hat{\mathbf{x}}^{(adv)}$	$\hat{\mathbf{x}}^{(cf \setminus c)}$	$\hat{\mathbf{x}}^{(cf \setminus v)}$
$\mathbf{c}_\downarrow(\mathbf{x}^*)$	0.4	0.5	0.0	4.4	0.5
$\mathbf{c}_\downarrow(\hat{\mathbf{x}}^{(cf)})$	-	0.2	0.4	4.4	0.2
\mathbf{v}_\uparrow	100	100	75	100	12
\mathbf{f}_\downarrow	2.5	2.6	3.0	2.8	2.5

Table 11: CelebA class *smiling* - Original examples \mathbf{x}^* compared to counterfactuals $\hat{\mathbf{x}}^{(cf)}$, adversarial examples $\hat{\mathbf{x}}^{(adv)}$ and XAIDIFF generations with closeness $\hat{\mathbf{x}}^{(cf \setminus c)}$ and validity factors $\hat{\mathbf{x}}^{(cf \setminus v)}$ disabled. No standard deviation for brevity.

\mathbf{x}^*	$\hat{\mathbf{x}}^{(cf)}$	$\hat{\mathbf{x}}^{(aff)}$

Table 12: Original examples \mathbf{x}^* compared to counterfactuals $\hat{\mathbf{x}}^{(cf)}$ and affirmative explanations $\hat{\mathbf{x}}^{(aff)}$ generated by XAIDIFF for the first 16 images of the CelebA train set and with the target class the class *eyeglasses*.

metrics	\mathbf{x}^*	$\hat{\mathbf{x}}^{(cf)}$	$\hat{\mathbf{x}}^{(aff)}$
$\mathbf{c}_\downarrow(\mathbf{x}^*)$	-	0.7 (0.2)	0.8 (0.2)
$\mathbf{c}_\downarrow(\hat{\mathbf{x}}^{(cf)})$	-	-	0.3 (0.1)
\mathbf{v}_\uparrow	-	99.5 (0.5)	99.6 (0.5)
\mathbf{f}_\downarrow	2.9 (0.3)	2.6 (0.2)	2.6 (0.2)

Table 13: Counterfactual explanations and affirmative explanations of the class *eyeglasses* for the first 16 images of the CelebA train set.

\mathbf{x}^*	$\hat{\mathbf{x}}^{(cf)}$	$\hat{\mathbf{x}}^{(aff)}$	$\hat{\mathbf{x}}^{(adv)}$	$\hat{\mathbf{x}}^{(cf\setminus c)}$	$\hat{\mathbf{x}}^{(cf\setminus v)}$

Table 14: MNIST original examples \mathbf{x}^* compared to counterfactuals $\hat{\mathbf{x}}^{(cf)}$, adversarial examples $\hat{\mathbf{x}}^{(adv)}$ and XAIDIFF generations with closeness $\hat{\mathbf{x}}^{(cf\setminus c)}$ and validity factors $\hat{\mathbf{x}}^{(cf\setminus v)}$ disabled. Red color corresponds to the classifier neither predicting the original, not the target class in the multi-class setting. Class *four* is y_o and class *nine* is y_t .

	\mathbf{x}^*	$\hat{\mathbf{x}}^{(cf)}$	$\hat{\mathbf{x}}^{(aff)}$
$\mathbf{c}_\downarrow(\mathbf{x}^*)$	-	1.3 (0.5)	1.3 (0.5)
$\mathbf{c}_\downarrow(\hat{\mathbf{x}}^{(cf)})$	-	-	0.5 (0.1)
\mathbf{v}_\uparrow	-	100.0 (0.0)	96.4 (12.6)
\mathbf{f}_\downarrow	1.5 (0.1)	1.7 (0.3)	1.7 (0.3)
	$\hat{\mathbf{x}}^{(adv)}$	$\hat{\mathbf{x}}^{(cf\setminus c)}$	$\hat{\mathbf{x}}^{(cf\setminus v)}$
$\mathbf{c}_\downarrow(\mathbf{x}^*)$	0.3 (0.2)	2.8 (0.8)	1.5 (0.6)
$\mathbf{c}_\downarrow(\hat{\mathbf{x}}^{(cf)})$	1.4 (0.5)	2.1 (1.0)	1.2 (0.5)
\mathbf{v}_\uparrow	97.1 (9.1)	60.8 (49.0)	12.5 (34.2)
\mathbf{f}_\downarrow	8.4 (2.7)	1.8 (0.3)	1.7 (0.3)

Table 15: MNIST metrics for original examples \mathbf{x}^* compared to counterfactuals $\hat{\mathbf{x}}^{(cf)}$, adversarial examples $\hat{\mathbf{x}}^{(adv)}$ and XAIDIFF generations with closeness $\hat{\mathbf{x}}^{(cf\setminus c)}$ and validity factors $\hat{\mathbf{x}}^{(cf\setminus v)}$ disabled. Class *four* is y_o and class *nine* is y_t .